Available online at www.sciencedirect.com
SCIENCE DIRECT
Thin Solid Films 488 (2005) 194 – 199
thin solid films
www.elsevier.com/locate/tsf

Properties of anatase $Co_xTi_{1-x}O_2$ thin films epitaxially grown by reactive sputtering

B.-S. Jeong[a], Y.W. Heo[a], D.P. Norton[a,*], A.F. Hebard[b], J.D. Budai[c], Y.D. Park[d]

[a]University of Florida, Dept. of Materials Science and Engineering, 100 Rhines Hall, P.O. Box 116400, Gainesville, FL 32611, USA
[b]University of Florida, Dept. of Physics, Gainesville, FL 32611-8440, USA
[c]Oak Ridge National Laboratory, Solid State Division, Oak Ridge, TN 37831, USA
[d]Seoul National University, School of Physics, Seoul 151-747, Korea

Received 29 October 2003; received in revised form 8 April 2005; accepted 8 April 2005
Available online 16 June 2005

Abstract

Epitaxial $Co_xTi_{1-x}O_2$ anatase thin films were grown on (001)$LaAlO_3$ by a reactive RF magnetron co-sputter deposition with water vapor serving as the oxidant. The use of water as the oxygen source proves useful in growing oxygen-deficient, semiconducting $Co_xTi_{1-x}O_2$ by reactive sputter deposition, with undoped and Co-doped TiO_2 thin films showing n-type semiconductor behavior, with carrier concentrations of $10^{17}-10^{18}$ cm^{-3}. Magnetization measurements of $Co_xTi_{1-x}O_2$ ($x=0.07$) thin films reveal ferromagnetic behavior in M-H loop at room temperature with a saturation magnetization on the order of 0.7 Bohr magnetons/Co. X-ray photoemission spectrometry indicates that the Co cations are in the Co^{2+} valence state. However, chemical analysis of surface structure indicates that a significant fraction of the cobalt segregates into a Co–Ti–O phase. This suggests that the ferromagnetic moments may reside in oxygen-bound Co that is segregated from the majority anatase phase.

PACS: 72.25.Dc; 81.15.Cd
Keywords: Titanium oxide; Magnetic structures; Sputtering

1. Introduction

In recent years, there has emerged considerable interest in the properties of transition metal doped semiconductors in an effort to develop electronics based on the spin of electrons. One approach to realizing novel spin-based electronic devices involves the exploitation of spin-polarized electron distributions in dilute magnetic semiconductor (DMS) materials. In most semiconductors doped with transition metals, the magnetic behavior, if any, is observed at temperatures well below room temperature [1–5]. Among the conventional semiconductors, (Ga, Mn)As exhibits the highest Curie temperature (Tc), on the order of 110 K [6,7]. In recent years, it has been reported that cobalt-doped semiconducting anatase (TiO_2) is ferromagnetic at room temperature [8]. This may provide for the development of spin-based DMS electronics that operate at room temperature if the ferromagnetic spin moments are present in the free electron distribution. Ferromagnetic thin films of $Co_xTi_{1-x}O_2$, epitaxially stabilized in the anatase structure, have previously been realized on $SrTiO_3$(001) and $LaAlO_3$(001) by pulsed laser deposition (PLD) and oxygen plasma assisted molecular-beam epitaxy (MBE) [8,9]. Spectroscopic studies on the MBE-grown TiO_2 thin films suggests that the cobalt exists in the Co^{2+} oxidation which is consistent with ferromagnetism originating from Co substitution on the Ti site. However, other studies of Co-doped TiO_2 films deposited by pulsed laser deposition suggest that the formation of Co nanoclusters may be responsible for the ferromagnetic properties [10]. Thus, it remains an open question as to the probable role that the specific processing technique plays in yielding these results.

* Corresponding author.
E-mail address: dnort@mse.ufl.edu (D.P. Norton).

0040-6090/$ - see front matter © 2005 Elsevier B.V. All rights reserved.
doi:10.1016/j.tsf.2005.04.113

In this paper, we report on the growth and properties of Co-doped TiO_2($Co_xTi_{1-x}O_2$) epitaxial thin films realized by reactive co-sputter deposition. The use of water vapor (H_2O) as the oxidant facilitates the formation of carriers via the creation of oxygen vacancies. We have previously reported on the transport properties of undoped semiconducting in transparent anatase TiO_2 thin films epitaxially grown by reactive sputtering deposition employing water vapor [11]. The primary focus of the present study is to investigate the properties of sputter-deposited $Co_xTi_{1-x}O_2$, with particular attention given to delineating the chemical state and substitutional behavior of Co in the TiO_2 matrix.

2. Experimental details

$Co_xTi_{1-x}O_2$ anatase films were epitaxially grown by a reactive RF magnetron co-sputter deposition with cation sputtering targets of Ti (99.995%) and Co (99.95%). The film-growth system was equipped with multiple 2″ sputtering sources and a load-lock for substrate exchange. The base pressure of the deposition system was on the order of 5×10^{-8} Torr. For epitaxially stabilized anatase TiO_2 film growth, (001) $LaAlO_3$ was chosen as the substrate as it provides a lattice mismatch on the order of 2 at.%. The substrates were cleaned in trichloroethylene, acetone, and methanol prior to loading on the sample holder. Argon was provided as the sputter gas. A water source was created by freezing and evacuating a water-filled stainless cylinder that was attached to the deposition chamber via a leak valve. The total pressure during growth was fixed at 15 mTorr, whereas the water vapor pressure was varied from 10^{-4} and 10^{-2} Torr. A water vapor pressure of $P(H_2O)=10^{-3}$ Torr was found to be optimal in realizing oxygen deficiency and semiconductor transport behavior. A substrate temperature during the deposition of 650 °C resulted in the growth of highly crystalline epitaxial Co-doped TiO_2 thin films in the anatase phase. The growth rate was on the order of 2 nm/min. Total film thickness ranged from 200 to 500 nm.

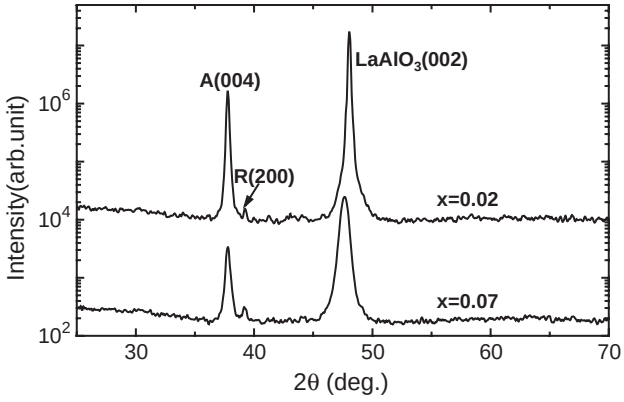

Fig. 1. The X-ray diffraction pattern for $Co_xTi_{1-x}O_2$ on $LaAlO_3$(001) ($x=0.07$, 0.02).

Table 1
Hall effect measurement for $Co_xTi_{1-x}O_2$ thin film ($x=0.07$, 0.02, 0)

	$Co_{0.07}Ti_{0.93}O_2$	$Co_{0.02}Ti_{0.98}O_2$	TiO_2 (undoped)
Resistivity (Ω cm)	7.18	0.186	0.283
Hall coefficient (cm^3/C)	−8.39	−4.18	−8.85
Hall mobility (cm^2/Vs)	1	22	31
Carrier concentration (cm^{-3})	8.09×10^{17}	1.48×10^{18}	7.46×10^{17}
Type	N-type	N-type	N-type

Hall effect measurement was performed with current at 100 μA, temperature at 300 K.

The crystalline structure of the Co-doped TiO_2 films was characterized by X-ray diffraction (XRD) with a Cu Ka radiation source. The diffraction patterns were taken with a Philips MRD X'Pert System. The samples were characterized as deposited with no pre-cleaning prior to measurements. Quantitative analysis of chemical composition was performed by electron probe microanalysis and Auger electron spectroscopy (AES). In order to extract information regarding chemical states of the element, X-ray photoelectron spectroscopy (XPS) was used with Al-Kα radiation

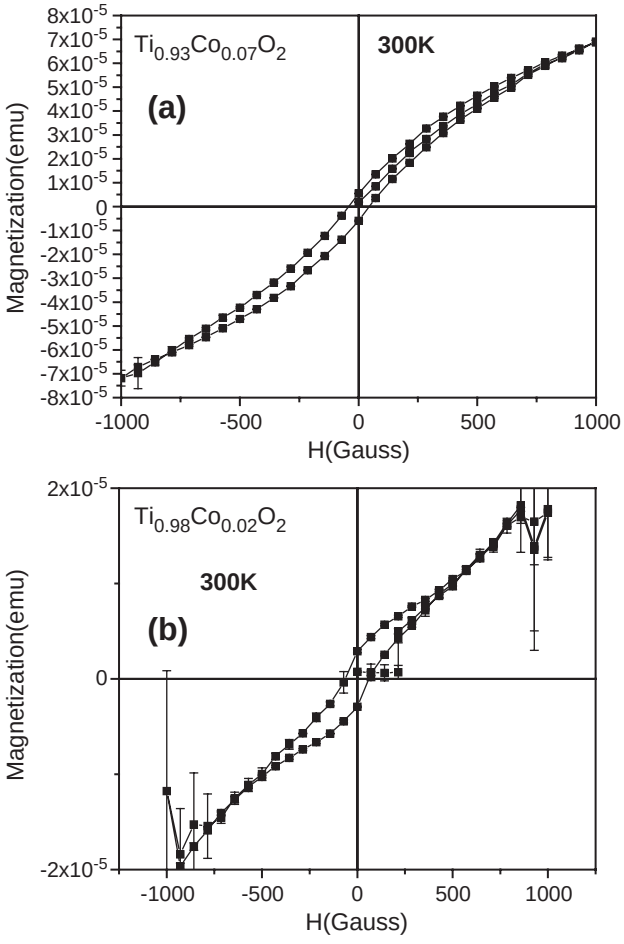

Fig. 2. M-H curves for $Co_xTi_{1-x}O_2$ thin films on $LaAlO_3$(001) with (a) $x=0.07$ and (b) $x=0.02$ taken at room temperature. Magnetic field was applied parallel to the film surface.

($h\nu$=1486.6 eV). A Perkin-Elmer Model 5100 X-ray Photoelectron Spectrometer was used. Samples were loaded into the UHV analysis chamber via a load-lock. There was no solvent or aqueous cleaning procedure for XPS or AES samples prior to mounting in the load-lock. The surface morphology, backscattered images and chemical mapping were performed by field emission scanning electron microscopy (FESEM) using a JEOL JSM-6335F. Auger electron spectrometry was performed using a Perkin-Elmer Model 660 Scanning Auger Electron Spectrometer. For both AES and XPS, the samples were sputter cleaned in situ prior to data acquisition. Hall effect measurements were performed to measure transport properties of oxygen-deficient Co-doped TiO_2 anatase films. An 8000 gauss magnetic field was used for these experiments. Room temperature magnetization was measured by a Quantum Design superconducting quantum interference device (SQUID) magnetometer for films with different Co content (x=0.07, 0.02).

3. Results and discussion

The Co-doped epitaxial anatase films realized for a growth temperature of 650 °C and water vapor pressure at 10^{-3} Torr exhibited crystalline quality similar to that seen in previous work on undoped films [12]. Fig. 1 shows the θ–2θ X-ray diffraction data taken along the surface normal for films deposited under these conditions with 2 at.% and 7 at.% Co doping levels. The films are near single phase epitaxial anatase with a small amount of secondary rutile phase seen in the data. From in-plane and out-of-plane X-ray diffraction measurement, the anatase lattice parameters were a=3.790 Å and c=9.495 Å. As shown in Fig. 1, there was no evidence for metallic Co or cobalt oxides phases seen in the diffraction data. This does not preclude the presence of the secondary phases since a small volume fraction of a randomly oriented impurity phase would be difficult to detect. However, metallic Co has been observed in X-ray diffraction scans of Co-doped ZnO. There is little difference observed for the X-ray diffraction patterns for these 2 at.% and 7 at.% doped films.

Table 1 shows the results from room temperature Hall effect measurements for the $Co_xTi_{1-x}O_2$ (x=0.07, 0.02, 0) thin films. The current used for the measurement was 100 μA. Both doped and pure anatase TiO_2 thin films show n-type semiconductor behavior. The carrier concentration was typically in the range 10^{17}–10^{18} cm^{-3}, which is lower than that shown for MBE-grown films [13]. The resistivity of the 7 at.% Co-doped thin film is slightly higher than that for doped or undoped anatase films. The carrier mobility clearly decreases as the cobalt concentration is increased. However, we note that the carrier concentration in these materials is not strongly dependent of Co concentration. If the majority of the Co ions substituted on Ti sites, one would expect a significant reduction of the electron concentration, assuming that Co retains a valence state of +2 or +3. This is not observed, suggesting that much of the cobalt must go elsewhere.

The SQUID magnetization properties of the Co-doped films are shown via the M-H plots shown in Fig. 2. For both

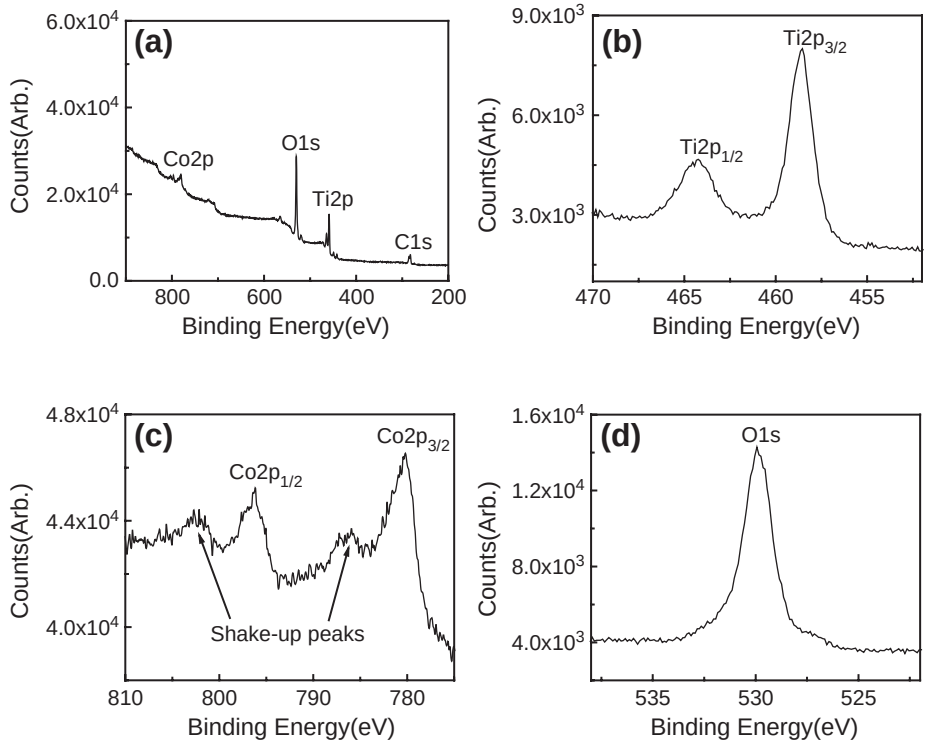

Fig. 3. XPS spectrum of $Co_{0.07}Ti_{0.93}O_2$ on $LaAlO_3$(001): (a) general spectrum, (b) Ti 2p band, (c) Co 2p band, (d) O 1s band.

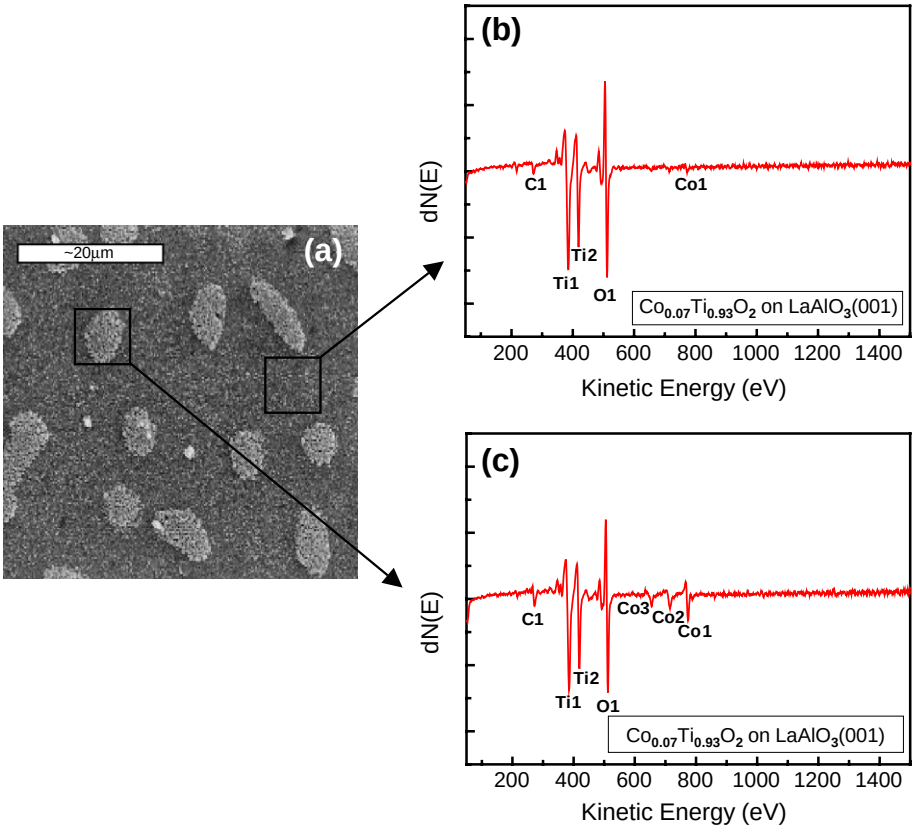

Fig. 4. Backscattered image and AES survey for the surface of $Co_{0.07}Ti_{0.93}O_2$ on $LaAlO_3$(001): (a) backscattered image, (b,c) AES survey.

the 7 at.% (Fig. 2a) and 2 at.% (Fig. 2b) Co-doped TiO_2 samples, hysteresis loops are observed at room temperature for film grown at 650 °C with water vapor as a oxidant. Clearly, the 7 at.% Co-doped TiO_2 film exhibits stronger ferromagnetic behavior relative to the 2 at.% doped sample. These results are consistent with both the MBE and PLD results reported earlier [9,10].

The elemental composition for the Co-doped TiO_2 thin films was determined by XPS. An XPS spectrum for the $Co_{0.07}Ti_{0.93}O_2$ film is shown in Fig. 3. The following peaks are observed in Fig. 3a: Ti 2p1 at 464.24 eV and Ti 2p3 at 458.49 eV, Co 2p1 at 796.21 eV and Co 2p3 at 780.12 eV, O 1 s at 529.9 eV and a carbon peak (C 1 s at 285.16 eV). The shift in all peaks caused by charging effects has been corrected using the standard peak, O 1s at 529.9 eV from TiO_2, as a reference as seen in Fig. 3d. The oxidation and spin state of the Ti atoms shown in Fig. 3b match well with standard Ti 2p1 and Ti 2p3 peaks, indicating that these two peaks correspond to Ti^{+4} from TiO_2 thin films [14]. The line separation between Ti 2p1/2 and Ti 2p3/2 was 5.75 eV, which is consistent with 5.7 eV as the standard binding energy. For the Co-related peaks shown in Fig. 3c, the oxidation and spin state of the Co atoms can be inferred from the shape of the Co 2p lines. The satellite peak structure that is observed on the high binding energy side of the principal 2p1/2 and 2p3/2 lines is indicative of high spin Co^{2+} [14]. The shake-up peak is a more easily identified characteristic of the chemical state of the Co than either the absolute binding energy or the line separation between Co $2p_{1/2}$ and Co $2p_{3/2}$ [15]. The results from the XPS analysis taken from the as-grown surface is consistent with the Co existing in the +2 formal oxidation state in these sputter-deposited $Co_xTi_{1-x}O_2$ anatase thin films. However, as reported by A. Rizzetti et al., it should be noted that small peaks corresponding to unoxidized cobalt are observed in the $Co_xTi_{1-x}O_2$ film subjected to a 4 min sputtering treatment with Ar ions. This Co likely results from reducing

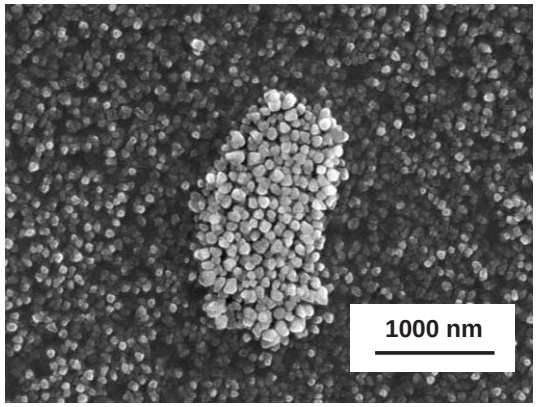

Fig. 5. Backscattered image of precipitates on $Co_{0.07}Ti_{0.93}O_2$ on $LaAlO_3$(001).

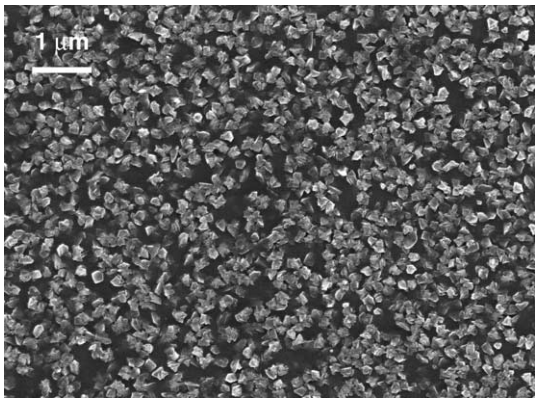

Fig. 6. Backscattered image of $Co_{0.02}Ti_{0.98}O_2$ on $LaAlO_3$(001).

the oxidized Co via Ar ion bombardment [16]. However, we cannot rule out the possibility that Ar ion sputtering reveals some metallic cobalt that exists in film.

In order to further investigate the properties of these materials, the surface topography and chemistry was determined using field-emission scanning electron microscopy with energy dispersive spectrometry.

Fig. 4 shows the backscattered electron image obtained by the FESEM and the result of auger electron spectroscopy survey for the surface of 7 at.% Co-doped TiO_2 anatase thin films grown on (001)$LaAlO_3$. The sample surface is decorated with apparent secondary phase precipitates. Fig. 5 shows an enlarged image of a precipitate cluster, which is approximately 1 μm in diameter consisting of small 100 nm diameter grains. As shown in Fig. 6, however, sputter deposited undoped TiO_2 and $Co_{0.02}Ti_{0.98}O_2$ films do not show these secondary phase precipitates, indicating that precipitate formation directly correlates with Co concentration. In order to further investigate these precipitates, selected area Auger electron spectroscopy was also performed. Results from AES, also given in Fig. 4, indicate that the Co dopant is principally located in the precipitate, with significantly less Co located in the film region between the precipitates. The intensity of the Co AES peak in the precipitate is at least fives times that for the Auger signal for the TiO_2 film. This appears consistent with the segregated Ti–Co–O particles which have been observed in MBE grown Co-doped films [13,17].

In order to further elucidate the composition of these precipitates, we employed spatial chemical mapping using energy dispersive spectrometry in the FESEM for the Co-doped TiO_2 film ($x=0.07$). Fig. 7 shows the intensity of each element peak plotted as a line scan across the Co-doped TiO_2 film surface ($x=0.07$). First note that the Ti and oxygen peaks were uniformly distributed across the film surface. If the secondary phase was Co metal, we would expect a drop in Ti signal intensity in the precipitates relative to the remainder of the films. This is not observed. However, when the Co signal is mapped, the secondary phase particles clearly contain higher Co content than the TiO_2 film area between the particles. These results indicate that the secondary precipitates are a Ti–Co–O phase, which is consistent with the results for MBE-grown films [9,13]. Note also that the secondary phase particles are brighter in the backscattered SEM image, indicating a somewhat insulating behavior. Co particles would be metallic. Note also that the oxygen peak intensity is somewhat higher in the segregation areas as well. From the surface structure and the result of XPS measurement, we conclude that the material of surface segregation in Co-doped TiO_2 thin films is Ti–Co–O particles.

In conclusion, we have investigated ferromagnetism in semiconducting anatase Co-doped TiO_2 thin films grown by

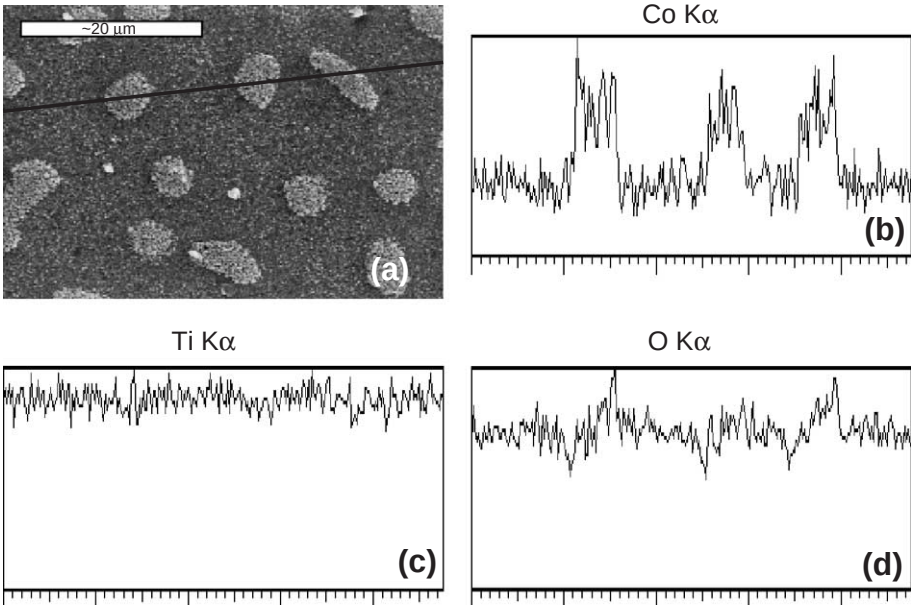

Fig. 7. BSE image and line scan of $Co_{0.07}Ti_{0.93}O_2$: (a) BSE image, (b) line scan for Co, (c) line scan for Ti, (d) line scan for O.

the reactive sputter deposition technique. Surface segregation from Co oxide particles was observed in highly doped films. Both pure and doped films grown using water vapor source showed n-type semiconductor properties. Our results from XPS clearly show that Co is primarily in the +2 formal oxidation state in these doped thin films. Further activities will focus on the origin of the ferromagnetism.

Acknowledgement

This work was partially supported by the Army Research Office through research grant DAAD 19-01-1-1508. The authors would also like to acknowledge the staff of the Major Analytical Instrumentation Center, Department of Materials Science and Engineering, University of Florida, for their assistance with this work.

References

[1] S. Datta, B. Das, Appl. Phys. Lett. 56 (1990) 665.
[2] S.A. Wolf, D.D. Awschalom, R.A. Buhrman, J.M. Daughton, S. Von Molnar, M.L. Roukes, A.Y. Chtchelkanova, D.M. Treger, Science 294 (2001) 1488.
[3] D.D. Awschalom, M.E. Flatté, N. Samarth, Scientific American, 2002 (June).
[4] S.A. Wolf, D.D. Awschalom, R.A. Buhrman, J.M. Daughton, S. von Molnar, M.L. Roukes, A.Y. Chtchelkanova, Science 294 (2001) 1488.
[5] Y.D. Park, A.T. Hanbicki, S.C. Erwin, C.S. Hellberg, J.M. Sullivan, J.E. Matson, T.F. Ambrose, A. Wilson, G. Spanos, B.T. Jonker, Science 295 (2002) 651.
[6] H. Ohno, F. Matskura, T. Omiya, N. Akiba, J. Appl. Phys. 85 (1999) 4277.
[7] H. Ohno, A. Shen, F. Matsukura, A. Oiwa, A. Endo, S. Katsumoto, Y. Iye, Appl. Phys. Lett. 69 (3) (1996) 363.
[8] Y. Matsumoto, M. Murakami, T. Shono, T. Hasegawa, T. Fukumura, M. Kawasaki, P. Ahmet, T. Chikyow, S.-Y. Koshihara, H. Koinuma, Science 291 (2001) 854.
[9] S.A. Chambers, C.M. Wang, S. Thevuthasan, T. Droubay, D.E. McCready, A.S. Lea, V. Shutthanandan, C.F. Windisch Jr., Thin Solid Films 418 (2) (2002) 197.
[10] D.H. Kim, J.S. Yang, K.W. Lee, S.D. Bu, T.W. Noh, S.-J. Oh, Y.-W. Kim, J.-S. Chung, H. Tanaka, H.Y. Lee, T. Kawai, Appl. Phys. Lett. 81 (2002) 2421.
[11] B.-S. Jeong, D.P. Norton, J.D. Budai, G.E. Jellison Jr., Thin Solid Films 446 (1) (2004) 18.
[12] B.-S. Jeong, J.D. Budai, D.P. Norton, Thin Solid Films 422 (2002) 166.
[13] S.A. Chambers, S. Thevuthasan, R.F.C. Farrow, R.F. Marks, J.U. Thiele, L. Folks, M.G. Samant, A.J. Kellock, N. Ruzycki, D.L. Ederer, U. Diebold, Appl. Phys. Lett. 79 (2001) 3457.
[14] Handbook of X-ray photoelectron spectroscopy, physical electronics, (1995).
[15] S.N. Towle, J.R. Bargar, G.E. Brown Jr., G.A. Parks, J. Colloid Interface Sci. 187 (1997) 62.
[16] A. Rizzetti, J. Xhie, K. Sattler, D. Yamamoto, W. Pong, J. Electron Spectrosc. Relat. Phenom. 58 (1992) 359.
[17] X.J. Fan, M. Murakami, R. Takahasi, T. Koida, Y. Matsumoto, T. Hasegawa, T. Fukumura, M. Kawasaki, P. Ahmet, T. Chikyow, H. Koinuma, Mater. Res. Soc. Symp. Proc. 700 (2002) S2.7.1.